Available online at www.sciencedirect.com
SCIENCE DIRECT®
Acta Materialia 52 (2004) 821–832
Acta MATERIALIA
www.actamat-journals.com

In situ SEM-EBSD observations of the hcp to bcc phase transformation in commercially pure titanium

G.G.E. Seward [a,*], S. Celotto [b], D.J. Prior [a], J. Wheeler [a], R.C. Pond [b]

[a] Department of Earth Sciences, University of Liverpool, Liverpool L69 3GP, UK
[b] Materials Science and Engineering, Department of Engineering, University of Liverpool, Liverpool L69 3BX, UK

Received 7 July 2003; received in revised form 12 September 2003; accepted 13 October 2003

Abstract

This study presents in situ observations of the hcp (α) to bcc (β) phase transformation in commercially pure titanium at 882 °C using SEM imaging concurrent with crystal orientation determination using EBSD. Direct observations of the onset of the phase transformation are presented showing the early stages of the growth of β plates within α grains and allotriomorphic β along α–α grain boundaries. Intragranular β plates have a Burgers orientation relationship (OR) with the parent α grain and are lenticular in shape. These plates also have a tent surface relief and surface-traces consistent with habit planes predicted by the phenomenological theory of martensitic crystallography for pure titanium. These features suggest a military component to the growth mechanism. The β allotriomorphs have a Burgers OR with one of the α grains abutting at the boundary, but do not have surface relief characteristic of a military transformation. These are likely to grow by a civilian mechanism. The final stage of the transformation is a process of competitive growth of the two β forms, with the allotriomorphic β dominating by virtue of its faster moving α–β interfaces. Grain growth in the β stability field is more than an order of magnitude faster than that in the α field at temperatures near the phase transformation.

Keywords: Titanium; SEM; High temperature EBSD; Polymorphic phase transformation; In situ techniques

1. Introduction

Recent developments in scanning electron microscopy (SEM) are enabling important material processes to be studied in situ. For example, recovery, recrystallisation and grain growth have been investigated using instruments with specimen stages that can reach temperatures up to 500 °C [1,2]. In these experiments microstructural changes have been observed with good spatial resolution (order of 100 nm). Here, we report a study of phase transformation using a specially designed SEM instrument fitted with a stage that can heat specimens to temperatures in excess of 1000 °C [3]. Furthermore, by means of electron back-scatter diffraction (EBSD), high precision crystallographic data have been acquired concomitantly. We have used SEM imaging and EBSD analysis to examine the α (hcp) to β (bcc) transformation in commercially pure Ti which occurs at about 882 °C.

Titanium and its alloys are important engineering materials, and several other researchers have studied the α–β transformation [4–6], since the phase transformation provides a method of refining microstructure and therefore mechanical properties [7]. The crystallography of the two phases is commonly found to be related by the Burgers orientation relationship (OR) where close-packed planes $\{0001\}_\alpha/\{110\}_\beta$ and close packed directions $\langle 11\bar{2}0\rangle_\alpha/\langle 111\rangle_\beta$ are parallel [8]. However, all published observations concerning the Burgers OR in pure Ti are from the β to α transformation after cooling. Study of the α–β transformation in pure Ti requires in situ techniques since the β phase cannot be retained by slow cooling or quenching.

When orientation relations exist between structures in a phase transformation, identifying the multiplicity of crystallographically equivalent variants of a product

* Corresponding author. Tel.: +44-151-794-5202; fax: +44-151-794-5196.
E-mail address: gseward@liv.ac.uk (G.G.E. Seward).

1359-6454/$30.00 © 2003 Published by Elsevier Ltd on behalf of Acta Materialia Inc.
doi:10.1016/j.actamat.2003.10.049

that can arise is important to relate the textures before and after the transformation. In the case of the Burgers OR, six β variants can arise in any α grain on the up temperature transformation. Consequently, if the texture of the starting material is known, the texture after transformation can be predicted on the basis that every variant has the same probability of forming and the same volume. However, if some mechanism operates that suppresses certain variants during nucleation or growth, the final texture and microstructure will be modified with potentially detrimental consequences for material properties [7]. Studies of the bulk texture of deformed and transformed Ti sheets show that the modification in textures can be correlated to the Burgers OR, but not all six β variants were equally developed [9]. The resultant texture was interpreted in terms of variant selection, but no microstructural data were available to support this interpretation. Another study by Gey and Humbert [10] shows similar results using a restitution method to reconstruct β textures from the final α textures after the phase transformation. There is a lack of spatially resolved crystallographic data directly related to textural and microstructural development resulting from polymorphic phase transformations in titanium.

We are now able to observe the nucleation and competitive growth of the β phase in the parent α grains upon heating and assess the crystallographic OR between phases. We are also able to follow this transient microstructural state through to the completed transformation. This real time approach allows us to see where and suggests how the β phase development occurs, and more importantly, if we are to predict the effect of processing, how the early stages of the transformation process influence the final microstructure and texture.

2. Experimental

Two samples of rolled and annealed commercial purity titanium were investigated, with the compositions given in Table 1. One sample was a 2-mm thick sheet and the other a slab of 15 mm thickness. Sheet specimens were prepared with the sample normal (ND) perpendicular to the rolling plane, and the slab specimens with the sample ND parallel to the rolling direction. Experiments were performed on 8 mm^2 specimens that were about 1 mm thick. The specimen surfaces were prepared by standard metallographic techniques with a final polish using a 1:5 mixture of hydrogen peroxide and a colloidal silica suspension for several hours.

Experiments were performed in the recently developed CamScan X500 Crystal Probe scanning electron microscope, designed for optimised electron back-scatter diffraction (EBSD) analysis with in situ heating [3]. Typical operating parameters were 20 keV accelerating voltage, 10–20 nA beam current, and 15–20 nm spot size. Secondary electron imaging (SEI) was employed for observation of surface topographic features, and back-scatter electron imaging (BEI) utilising forward mounted detectors was employed for observation of crystal orientation contrast [11–13]. HKL software was used for EBSD acquisition and data manipulation. The heating stage was designed and built by Oxford Instruments (now trading as Gatan UK) and the Obducat CamScan development team specifically for the X500 [3].

During the in situ experiments the temperature is measured by a thermocouple in the furnace. The sample temperature is then derived using a calibration curve determined by preliminary experiments with a thermocouple welded to a titanium sample of similar geometry. The temperature of the samples was ramped up to about 870 °C, which is below that of the phase transformation. After holding for half an hour, the temperature was ramped through the phase transformation at a rate of 10 °C/min and held at 910 °C. The specimen is held in the observation position throughout the duration of an experiment so that imaging and EBSD analysis can be conducted continuously. The microstructural evolution of the specimen can be followed at temperatures above the phase transformation for many hours.

3. Results

3.1. Initial microstructure

The initial microstructure for both the sheet and slab materials consists of equiaxed polygonal α grains with an average grain size of about 50 μm. Using the standard rolling plane and direction convention for describing crystallographic textures, the materials have a predominant $\{2\bar{2}05\}\langle 11\bar{2}0\rangle$ component (see Fig. 8(a)), as expected for rolled and recrystallised titanium [14]. After heating up to and holding at a temperature just below the phase transformation, the $\{2\bar{2}05\}\langle 11\bar{2}0\rangle$ tex-

Table 1
Chemical composition of the slab and sheet materials in wt% except where stated otherwise

Sample	Al	Fe	H	N	O	V	Y	Others[a]
Slab	0.03	0.040	17 ppm	0.004	0.22	0.01	<0.001	<0.1
Sheet	<0.01	0.060	48 ppm	0.010	0.19	<0.01	<0.001	<0.1

[a] Others include Si, Mn, Co, Cr, Cu, Mo, Nb, Ni, W, Zr and Sn.

ture component showed a minor intensification and the average grain size increased to about 80 μm.

3.2. Initial appearance of β phase

In situ observations of the phase transformation show that the β phase nucleates and grows within the α grains and at the α/α grain boundaries at approximately the same time. The presence of β phase is confirmed using EBSD patterns collected from specific regions exhibiting changes of image contrast. One form of this contrast is due to surface relief features within the α grains like that shown in the SEI of Fig. 1(a). The other form is from thermal etching that formed microscopic crystallographic steps on the surface, as can be seen in the BEI of Fig. 2(a). Though thermal etching occurs in both phases, it is more pronounced in the β phase, as the inset BEI in Fig. 2(b) shows. The different extent of thermal etching seen in Figs. 1 and 2 for the sheet and slab materials, respectively, is because in the latter experiment slower heating rates and longer holding times were used, allowing the thermal etching to develop more.

3.3. Intragranular β plates

In general, within individual α grains several crystallographically distinct β phase variants have been observed to form and grow. For example, the lenticular contrast (labelled P) within the α grain of the slab material shown in the SEI of Fig. 1 shows that more than 10 separate β intragranular plates have formed. In some instances the β crystals (e.g. P1) have formed in parallel lenticular sets such as that in the top-left corner of the grain. In other instances they form a nested formation such as that in the centre (e.g. P3). These plates have a number of characteristic features in common. They all have a Burgers OR with the parent α grain as attested by the coincident $(0\,0\,0\,1)/\{1\,1\,0\}$ poles and $\langle 1\,1\,\bar{2}\,0\rangle/\langle 1\,1\,1\rangle$ directions shown in the associated pole-figures in Figs. 1(b)–(e) and 2(c). Note that P1 and P2 share the same $\{1\,1\,0\}$ poles and $\langle 1\,1\,1\rangle$ directions, but they are different variants because they are related by a $\{1\,1\,\bar{2}\,0\}$ α phase mirror plane, which is not a β phase mirror plane. The β plates are typically lenticular in shape with a characteristic contrast of bright/dark indicative of a tent-surface morphology. Note that in the image there is evidence for both tent (P2 and P3) and inverted tent (P1 and P4) relief. (When interpreting the contrast in terms of relief it should be noted that the incident beam is from the top of the image inclined 20° to the sample.) The surface trace of the β phase habit plane, defined by the mid-rib of the lens-form, is, within experimental error, consistent with the surface trace of a particular $\{3\,3\,4\}$ habit plane. The particular $\{3\,3\,4\}$ trace passes through the common $(0\,0\,0\,1)/\{1\,1\,0\}$ pole as can be seen

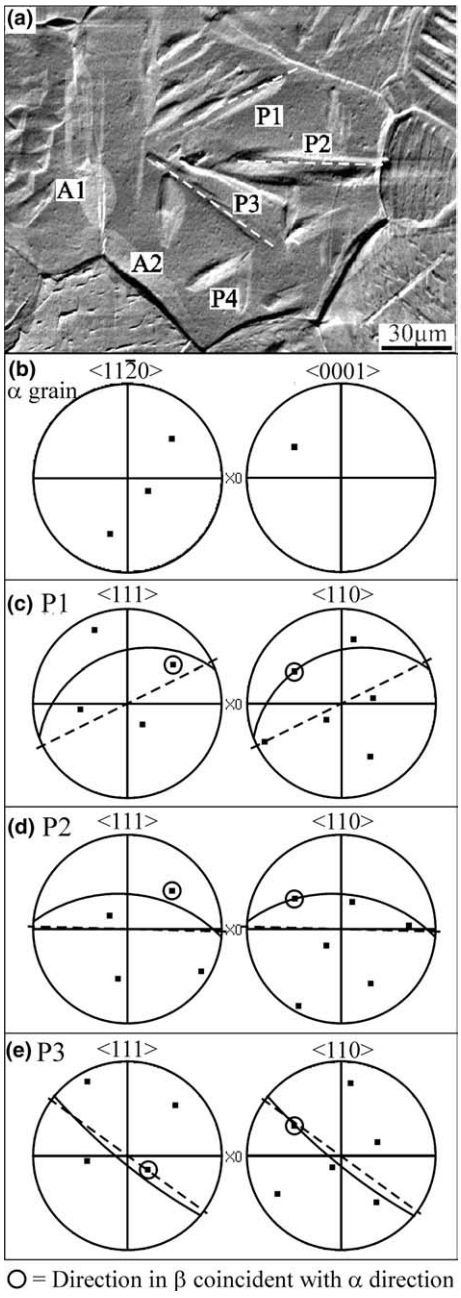

Fig. 1. A snapshot of the transient microstructure at ~882 °C where β crystals are forming within a α grain of the pure titanium slab, with (a) a SEI image with intragranular plates and grain boundary allotriomorphs indicated P and A, respectively, and stereographic projections (upper hemisphere); (b)–(e) giving the orientation of the parent α grain and intragranular plates P1, P2 and P3, respectively. The dashed lines and the arcs represent the habit plane surface trace and the corresponding $\{3\,3\,4\}$ plane, respectively.

in Figs. 1(b)–(e), and its pole is at an angle of 78.58° to the common $\langle 1\,1\,\bar{2}\,0\rangle/\langle 1\,1\,1\rangle$. This is shown in Fig. 3 together with the directions of the three measured surface traces after reorientation so as to correspond to the particular variant shown in the figure. The figure shows that all of the directions lie within ±5° to the $(3\,\bar{3}\,\bar{4})$

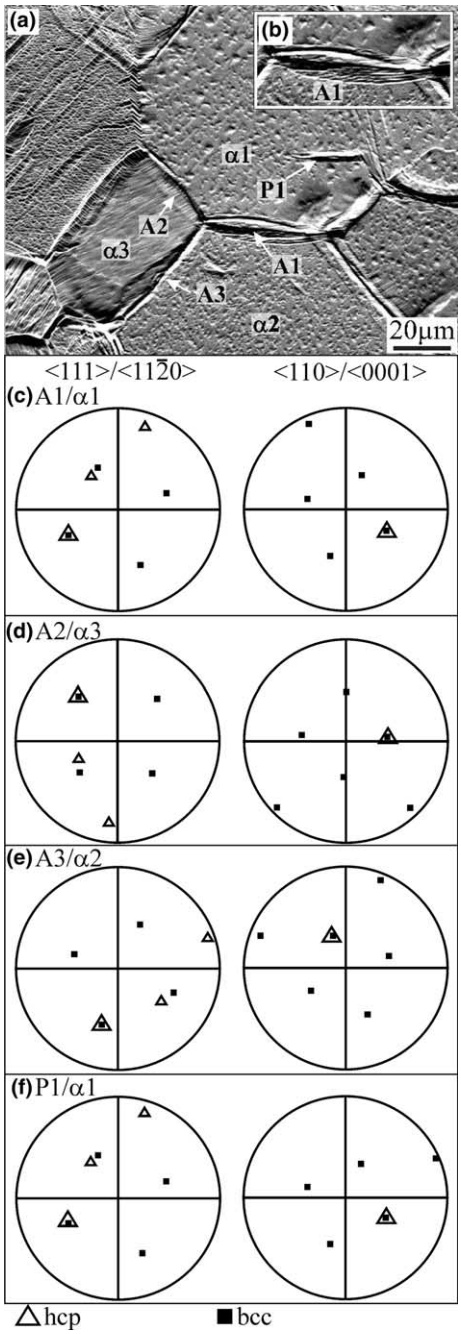

Fig. 2. A snapshot of the transient microstructure at ~882 °C where β crystals are forming within a α grain of the pure titanium sheet, with (a) a BEI image with grain boundary allotriomorphs and intragranular β crystals indicated A and P, respectively; (b) a enlarged section of the BEI to show the difference in thermal etching between the β and α phases, and with stereographic projections; (c)–(f) giving the orientation of the parent α grain, intergranular β plate and grain boundary β allotriomorphs P1, A1, A2, and A3, respectively. Note the Burgers OR is confirmed.

when the orientations are transferred to the specific Burgers OR $(0\,0\,0\,1)/(1\,1\,0)$ and $[1\,1\,\bar{2}\,0]/[1\,1\,1]$. Note that the aspect ratio of the plates corresponds well to the inclination of the particular $\{3\,3\,4\}$ habit plane with

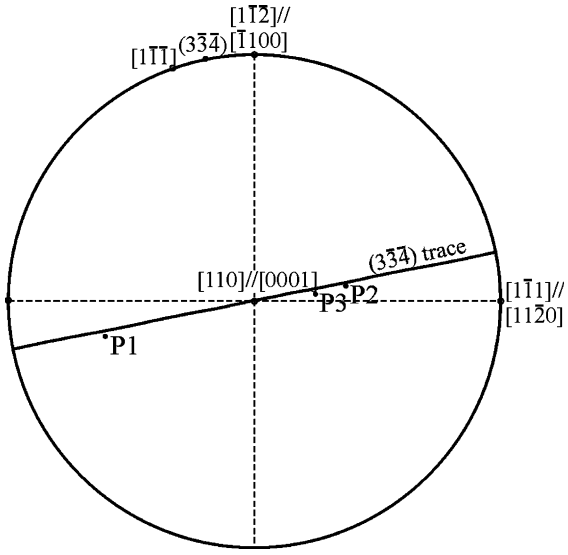

Fig. 3. A stereographic projection for the α–β Burgers OR showing the specific habit plane for pure Ti martensite given by the PTMC and the directions of the experimentally observed surface traces of the β intragranular plates shown in Fig. 1, which have rotated to correspond with the variant orientation shown.

respect to the surface (i.e. the smaller the ratio the greater the plane inclination).

3.4. Grain boundary β allotriomorphs

The β phase grows quickly along the α grain boundaries up to the triple junctions. Several examples are labelled A in the SEI and BEI of Figs. 1(a) and 2(a), respectively. In the examples shown in Fig. 1, the relatively low contrast between the β allotriomorphs and the α matrix is due to the difference in crystal structure rather than a difference in topography that SEI normally detects. The characteristics of the contrast indicate that the β allotriomorphs do not have a tent or any other kind of surface relief. The contrast associated with allotriomorphs in Fig. 2 arises due to enhanced thermal etching of the β phase and thermal grooving of the α grain boundaries prior to β formation.

The orientations of the intragranular plates and allotriomorphic β relative to the surrounding α grains, as determined from EBSD patterns taken during the phase transformation, are shown in Figs. 2(d)–(f). Comparison of α and β pole plots shows that the allotriomorphic β always has a Burgers OR with one of the neighbouring α grains. Not all of the α–α grain boundaries are decorated by allotriomorphic β as can be seen in Fig. 2(a). All of these α–α grain boundaries were high angle with no special rotation angles or disorientations. From the limited number of allotriomorphic β measured, there is no relationship evident between the presence or absence of allotriomorphic β on grain boundaries and α–α grain disorientations or α parent orientations.

3.5. β Grain growth

Fig. 4. shows a series of images acquired through time, during the final stages of the transformation. The images show that just prior to the appearance of large β grains, probably from below the surface, the α–β interfaces of the β allotriomorphs migrate away from the grain boundary. Fig. 5 shows β crystal orientation data from individual intragranular plates and grain boundary allotriomorphs measured during the transformation. All but one of the β allotriomorphs are oriented with ⟨100⟩ close to ND, whereas only one intragranular plate is consistent with that component. The overall distribution of orientations of the β allotriomorphs has cylindrical symmetry, which is especially clear in the ⟨110⟩ pole plot.

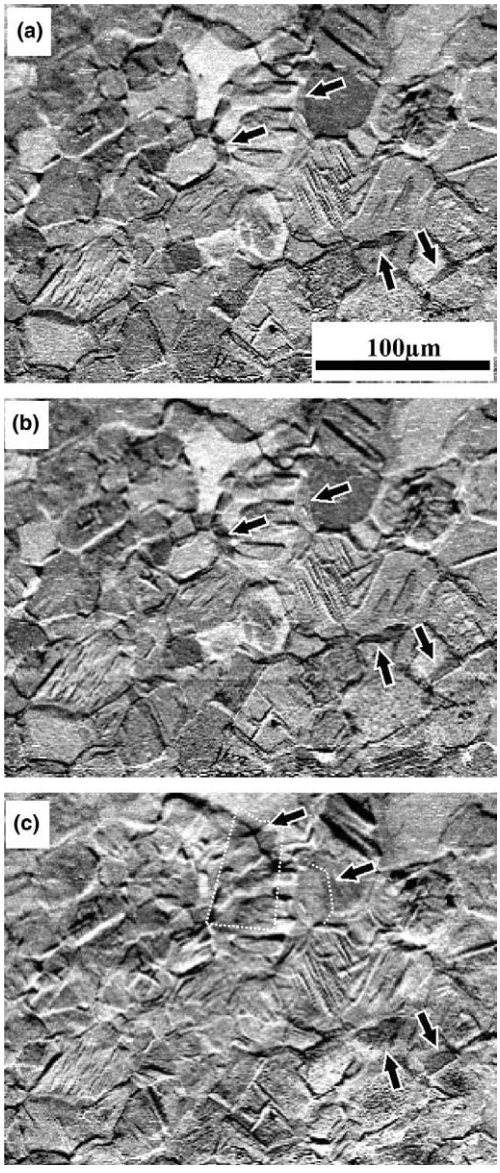

Fig. 4. A series of BEI images acquired at 2-min intervals during the final stages of the phase transformation. The arrows indicate mobile interphase boundaries of the β allotriomorphs. Just prior to the appearance of large β grains, probably from below the surface, the α–β interfaces of the β allotriomorphs migrate away from the grain boundary.

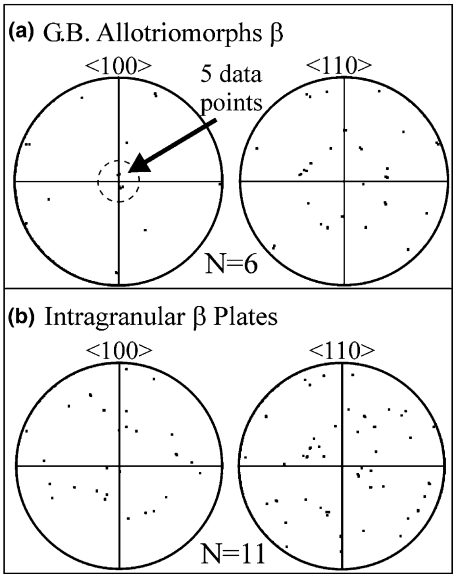

Fig. 5. Stereographic projections showing the β crystal orientation data from individual intergranular (a) and intragranular (b) polymorphs during the transformation.

The complete transformation of the α microstructure is not achieved through the coalescence of all existing β crystals, but by a small number of β grains with mobile boundaries that sweep through both transformed and untransformed materials, consuming smaller β crystals in the vicinity as indicated in Fig. 4. After the sample has fully transformed, grain growth of the β microstructure is rapid, forming large polygonal grains with dihedral angles close to 120°. Examples of this grain growth are illustrated in Fig. 6 for the slab material held at a temperature of about 910 °C for various times in different experiments. In the BEI images shown in Figs. 6(a) and (b), the large polygonal regions of various grey scales with average diameter >200 μm are β grains that are made visible by orientation contrast. Fig. 6(c) shows an optical micrograph of the specimen after cooling, where the optical effect from the thermal etching reveals the size of the β grains reached after 4 h at temperature, although the specimen is now transformed to α grains.

A comparison of the grain growth rates for α and β phases was performed from SEM image observations from different experiments. The average α grain size as a function of time was measured just below the phase transformation temperature at 870 °C and just above for the β at 910 °C. The two temperatures were within 40 °C of each other to make the comparison as direct as possible. The start time for the α data is taken to be when the specimen reached 870 °C and for the β data it was when the transformation was complete. The results

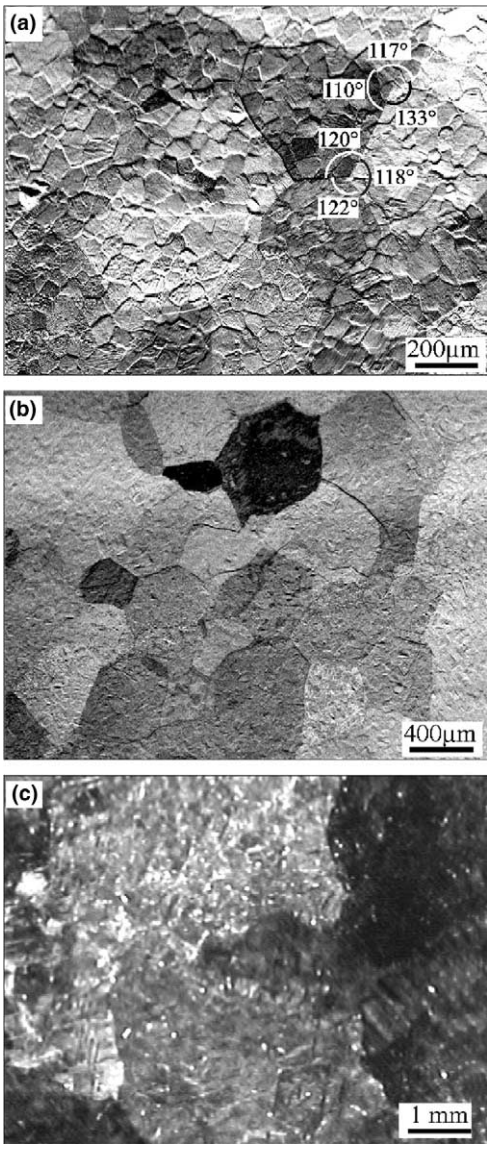

Fig. 6. The development of the large β grains after (a) 30 min, (b) 1 h and (c) 4 h at temperatures of about 910 °C. BEI are shown for both (a) and (b), there are number of contrast mechanisms operating associated with surface topography and crystal orientation. The pre-existing α microstructure of average grain size 30 μm can be seen from the contrast at the etched grain boundaries although no α phase is present. This etching occurred during the specimen preparation stages and from thermal grooving upon heating to the β phase field. The low take-off angle (20°) of the back-scattered electrons to the fore-scatter detectors make the BEI very sensitive to topography and thus, the initial α boundaries are still visible. (c) An optical image taken after cooling, where the optical effect from the thermal etching reveals the size of the β grains.

shown in Fig. 7 indicate that the β grain growth rate is at least an order of magnitude greater than that of the α for comparable grain size. It should be noted that the specimen size becomes an important and essentially limiting factor for the β grain growth since the diameters are of the order of millimetres at the end of the experiment when the whole specimen consisted of four grains.

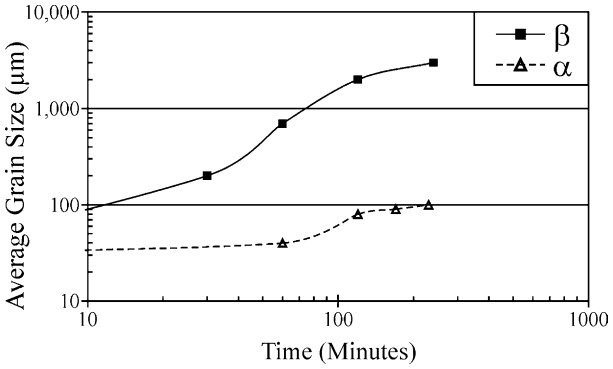

Fig. 7. A plot of the average grain size with time at temperature, both on logarithmic scales, for the α phase at 870 °C and β phase at 910 °C for different experiments.

3.6. Orientation data

After the phase transformation is complete, it is possible to determine directly the texture of the β phase at temperature by single measurements per grain or by standard orientation image mapping (OIM). Though sample dimensions of 8 × 8 mm with a β phase grain-size greater than 200 μm afford a limited grain population for analysis, most of the grain orientations within a sample can be measured. The measured β orientations are shown as contoured pole figures in Fig. 8(b) for the sheet material, with the α texture prior to the phase transformation for comparison shown in Fig. 8(a). All of these textures are for one point per grain, and individual data points are shown when data populations are small. The β texture shows a major $\{001\}\langle100\rangle$ component, and an additional minor component that has the $\langle111\rangle$ aligned in the RD.

For comparison, shown in Fig. 8(c) is a theoretical beta texture calculated from the same initial α texture. The theoretical texture has been generated by calculating six variants, via the Burgers OR for each grain in the α microstructure. The calculated texture is thus that which would be expected if there were no bias towards particular variant orientations during the transformation. Comparison of the theoretical and experimental textures indicates that the $\{001\}\langle100\rangle$ component is enhanced in the experimental data. However, particular crystallographic orientations can be selected from the theoretical texture to produce the observed $\{001\}\langle100\rangle$ component. Fig. 9 shows subgroups of variant orientations selected for which $\langle100\rangle$ is within 7.5° of ND (as indicated by the dashed circles at the centres of the $\langle100\rangle$ pole plots) for the theoretical and experimental data. Comparison of the distribution of orientations in Figs. 9(a) and (b) and 8(b) indicates that the experimental data are consistent with the Burgers OR being observed during transformation, with a variant selection biased towards $\{001\}\langle100\rangle$.

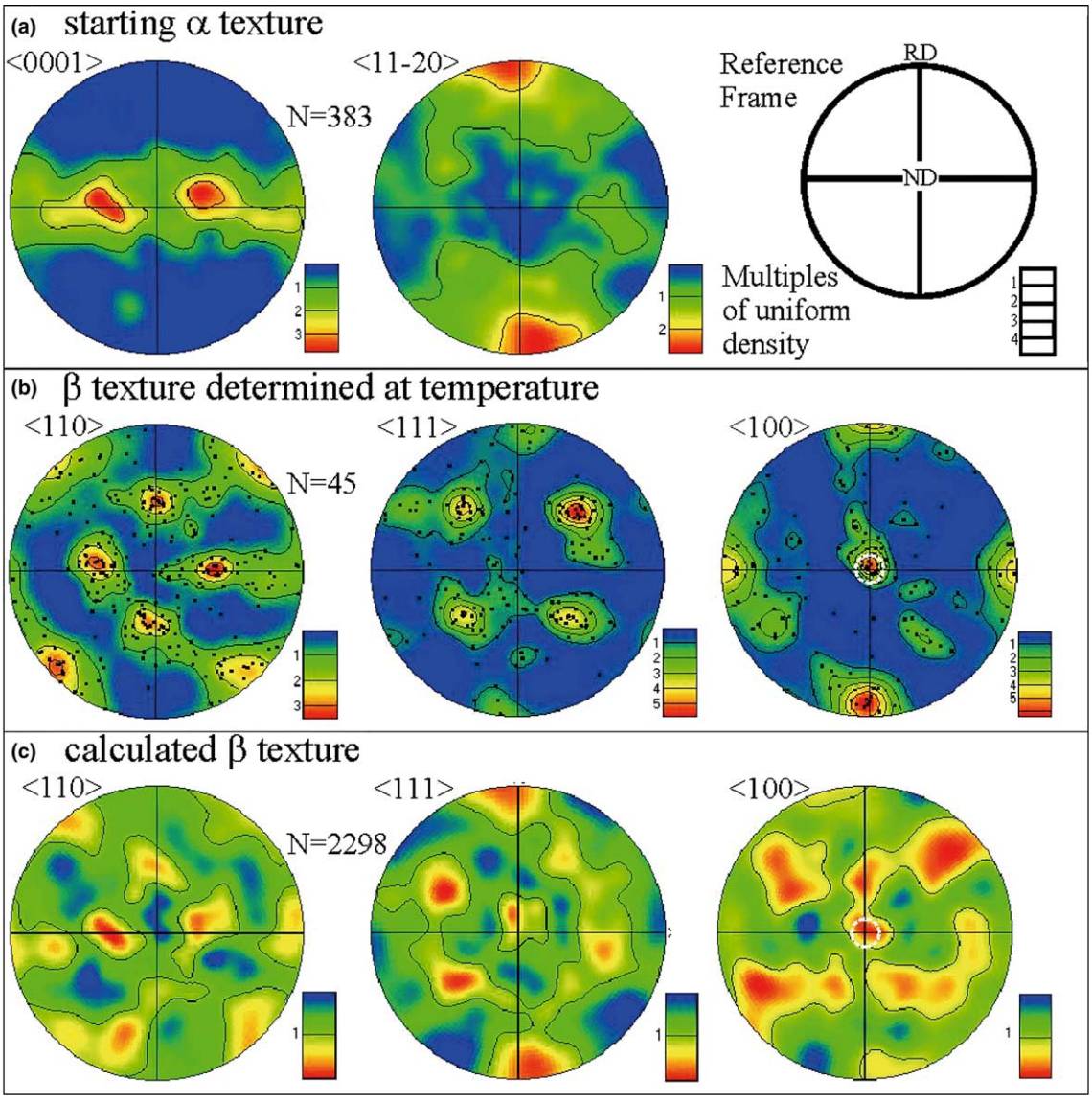

Fig. 8. Contoured pole figures showing the crystallographic textures of the sheet for (a) initial α phase microstructure, (b) β phase microstructure at temperature (c) theoretically derived β from initial α.

4. Discussion

The in situ observations of the α to β phase transformation demonstrate clearly that nucleation and growth of both intragranular plates and grain boundary allotriomorphs occurs. In all cases observed for both forms, orientated nucleation occurs with the Burgers OR. This suggests that the energy barrier for nuclei with the Burgers OR is relatively low compared to non-oriented nucleation. The mechanisms available for the subsequent growth of the nuclei will be determined in part by this orientation at the nucleation stage.

The kinetics of the growth of a nucleus is determined in part by its interfaces, and may be different for plate-like intragranular and allotriomorphic forms. Investigations of moving interphase interfaces using SEM cannot reveal their structure at the atomic level, but characteristic surface features arise that enable semi-coherent and incoherent interfaces to be distinguished. Disconnection (or transformation dislocation) movement along an interface couples shear-like displacement with interface motion (i.e. glide of the disconnection shears the parent lattice into the product, simultaneously advancing the interface), even if diffusional accommodation of misfit strains or composition change is also occurring [15]. As a result the phase transformation mechanism is inherently a military process (i.e. a coordinated motion of atoms crossing the interface as a disconnection passes), but the kinetics can be limited by bulk or interfacial diffusion. Consequently, if shear-like displacement effects the phase transformation, distinctive topographic features arise on the specimen surface

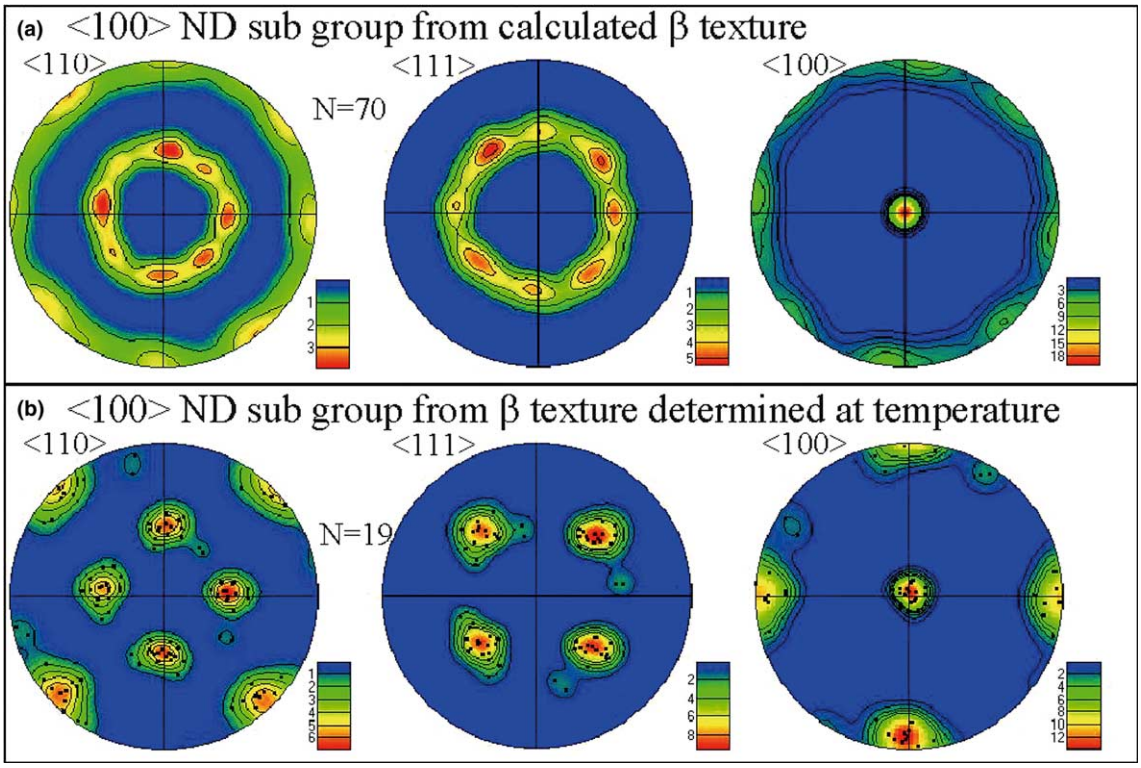

Fig. 9. Contoured pole figures showing the crystallographic texture of the β grain orientations subgroup with ⟨0 0 1⟩ in the ND selected within the circle at the centre of the pole figures in Fig. 8 for β textures (a) theoretically derived from initial α microstructure, and (b) that measured at temperature.

where transformation products emerge from below. Similarly, fiducial markers undergo characteristic deviations. These characteristic surface features are illustrated schematically in Fig. 10. In Fig. 10(a) the case of a product formed by an invariant plane transformation like that of martensite is shown [16], and 'tent' relief due to a single plate product is depicted in Fig. 10(b). It has been suggested that the origin of the latter is due to disconnections with different Burgers vectors, moving on opposite interfaces of a plate [17]. By this means, the overall shear exhibited by a plate can be reduced compared with that for an invariant plane product of similar dimensions. As a corollary, the shear strains around such plates can be more easily accommodated and

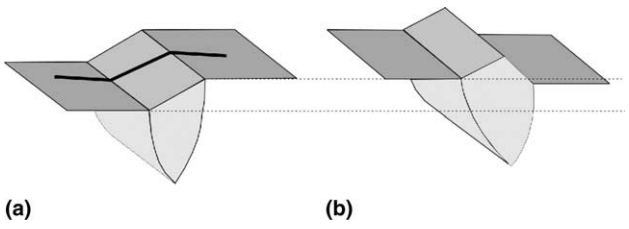

Fig. 10. Schematics of surface topography from (a) invariant plane transformations, also showing the effect on a fiducial marker, and (b) 'tent' relief due to a plate product.

growth of isolated plates is less affected by stress build up at the plate ends. In the present experiments, where the driving force for transformation is small (due to a small overstep of the transformation temperature) intragranular β plates of this type are anticipated.

4.1. Intragranular β plates

The in situ observations from this study show that multiple variants of β plates form in a given α grain and that the intragranular β plates exhibit surface topography characteristic of military phase transformation mechanisms. In addition, the surface traces of the habit planes are consistent with the phenomenological theory of martensitic crystallography (PTMC) [18–20]. This long established theory predicts the geometrically invariant plane between two crystal structures and shows that a particular habit plane exists for a particular variant of the orientation relationship. In the case of β to α in pure Ti the PTMC predicts the orientation relation to be close to the Burgers OR (with a deviation less than 2°) and the habit planes to be a particular {3 3 4} of the β crystal with respect to the orientation relationship [21]. The intragranular β plates exhibited both the Burger OR and surfaces traces consistent with the particular {3 3 4}.

Though the intragranular β plates exhibit morphological characteristics in common with military phase

transformation, the interface velocities are very different. The plates have an approximate interface velocity of 10^{-2} m/s based on the observation that it took 30 s to elongate to the size of 60 μm shown in Fig. 1. This is far less than the interface mobility of martensitic transformations, which can approach the speed of sound in the material (i.e. $\sim 10^3$ m/s) [22]. For truly martensitic behaviour, the interface structure must meet certain restrictive criteria, otherwise the transformation will require long-range diffusion of material to the disconnections, crystal defects at the interface, or disconnection/crystal-defect intersections [23,24]. This diffusion would ensure accommodation of the misfit strains parallel to the moving interface. Nevertheless, transformation by the motion of interfaces can still exhibit shear-like features because of the shear component of the disconnection, i.e. the dislocation component of the interfacial defect, while the kinetics is limited by diffusional accommodation to specific sites at the interface.

4.2. Grain boundary allotriomorphs

The grain boundary allotriomorphs exhibit no systematic surface topography or morphological features of military transformations like that of the intragranular plates, though they show the same oriented nucleation. After nucleation (regardless of whether this is on, or near to the grain boundary), a β allotriomorph grows along an α–α grain boundary and so its morphology is dominated by the orientation of the α–α grain boundary. At this stage it is unlikely that the interfaces will have the particular {3 3 4} habit plane that is required for the military transformation mechanism. Growth of the β phase is not then expected to result from the motion of disconnections (thus displaying no surface displacement), but to proceed by a 'civilian' or disorderly transport of atoms across the interface [16] (i.e. similar to the migration of a high angle grain boundary). The term massive transformation could be used to classify this type of transformation.

Summarising, while there is no difference in the compositions between the α and β phases, the characteristics of the intragranular plates and the grain boundary allotriomorphs show that each form grows by different mechanisms, the former with a shear or military component, and the latter with a civilian mechanism. Next it will be discussed how the difference in growth kinetics between these two mechanisms affects the final β phase texture.

4.3. Final texture

The dominant $\{0\,0\,1\}\langle 1\,0\,0\rangle$ texture component of the β phase is consistent with transformation from the starting α texture according to the Burgers OR with variant selection. Direct observation of β textures has been made by Zhu et al. [9] using high temperature XRD, three components reported are $\{0\,0\,1\}\langle 1\,0\,0\rangle$, $\{0\,0\,1\}\langle 1\,1\,0\rangle$ and $\{1\,1\,2\}\langle 1\,1\,0\rangle$. Gey and Humbert [10], using a restitution method to calculate β textures from post-transformation α textures, have calculated $\{0\,0\,1\}\langle 1\,0\,0\rangle$ and $\{1\,1\,2\}\langle 1\,1\,1\rangle$ components. However, both studies suggested that variant selection occurs in the α–β transformation only after rolling. These observations are consistent with the ideas of Furuhara and Maki [7] that suggest that the nucleation/selection of a particular variant is determined by dislocations and other crystal defects, even if the growth mechanism is a civilian process. In the present study, we are able to observe transient microstructures and quantify the crystallography during the phase transformation to assist in our understanding of variant selection processes.

Our in situ observations of intragranular plates show that several crystallographically distinct variants (at least 4 in Fig. 1(a)) are nucleated within a single parent α grain, suggesting there is no variant selection during nucleation in this material. Furthermore, for the intragranular plates there was no significant texture component with $\langle 1\,0\,0\rangle$ in the ND (see Fig. 5(b)) as there was for the grain boundary allotriomorphs (Fig. 5(a)) and for the final β texture (see Fig. 8(b)). This implies that the variant selection we observe in the final β texture is occurring by means of preferential nucleation and/or growth of the grain boundary allotriomorphs. Comparison of the texture symmetry for the grain boundary allotriomorphs in Fig. 5(a) with the final β texture Fig. 8(b) shows that further variant selection has taken place. While the β allotriomorph's texture has cylindrical symmetry with the $\langle 1\,0\,0\rangle$ parallel to the ND, the final β texture has in addition to this the $\langle 1\,0\,0\rangle$ parallel to the RD to give a cube texture. An explanation for the variant selection that causes the observed texture (also noted in [9,10]) is yet to be found.

For the grain boundary allotriomorphs to dominate in the final β texture, they must prevail over the intragranular plates during the growth stage. The interpretation of the observations in Fig. 4 is that the boundaries of the β allotriomorphs have greater mobility than those of the intragranular plates during the final stages of the transformation. Furthermore, since intragranular plates are not observed in the final β microstructure, these must have been engulfed by the surrounding allotriomorphs. This is shown schematically in Fig. 11. Since the intragranular plates within the allotriomorphs are the same β phase, the driving force for removing the plates cannot come from differences in chemical potential. However, the high curvature at the end of the plates (labelled 'r' in Fig. 11) will make such microstructural features unstable due to interface energy driving forces, once they are surrounded by β phase and cause these β–β grain boundaries to migrate as shown in the schematic.

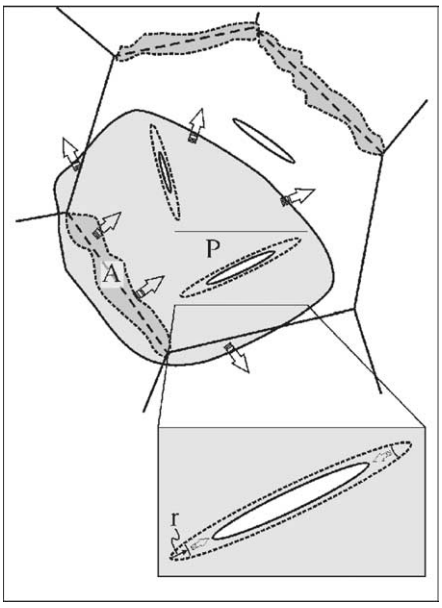

Fig. 11. Schematic of the competitive growth between intragranular plates and grain boundary allotriomorphs. The dark grey regions represent the growing β allotriomorphs. The arrows indicate the direction of the moving α–β interfaces between the β allotriomorphs and α matrix, and the β–β interfaces between the β allotriomorphs and intragranular plates.

4.4. Comparison of in situ SEM and vacuum furnace transformed samples

In situ heating in the SEM inherently involves observation of a free surface, and thus it is important to consider their influence on the phenomena studied. One approach is to section a larger volume sample that has been similarly heat-treated ex situ, and subsequently compare its internal and surface microstructures using SEM. Fig. 12 shows EBSD map data highlighting the results of applying this method. A sample of slab material with dimensions $10 \times 10 \times 8$ mm was used; this size enables the examination of an internal region that is at least 2α grain diameters distant from any surface. The surface and internal section in Figs. 12(a) and (c) show similar microstructures exhibiting large domains, each domain having a particular crystallographic orientation. Two types of domains are observed in Figs. 12(b) and (d): (i) regions like those marked A showing no clear substructure, and (ii) regions marked P showing parallel arrays of low-angle grain boundaries. A-domains correspond to allotriomorphic α regions, and a P-domain arises by coalescence of a stack of single-variant α plates which grew within a particular β grain. We infer that the large domains of similar orientation represent a minimum estimate of the grain size for the β phase microstructure prior to transformation. These observations show that the process of allotriomorphic growth is not restricted to the free surface. The deviations of dihedral angles from 120° observed in Fig. 12 (cf. Fig. 6) occur during β–α transformation, firstly because several crystallographically equivalent α plate variants can form in each β grain, and secondly because α allotriomorphs grow along β–β grain boundaries and expand into the neighbouring grains. It is this process that makes the determination of the prior β phase microstructure from the final alpha phase microstructure problematic, and also the reason why only a minimal estimate of the β

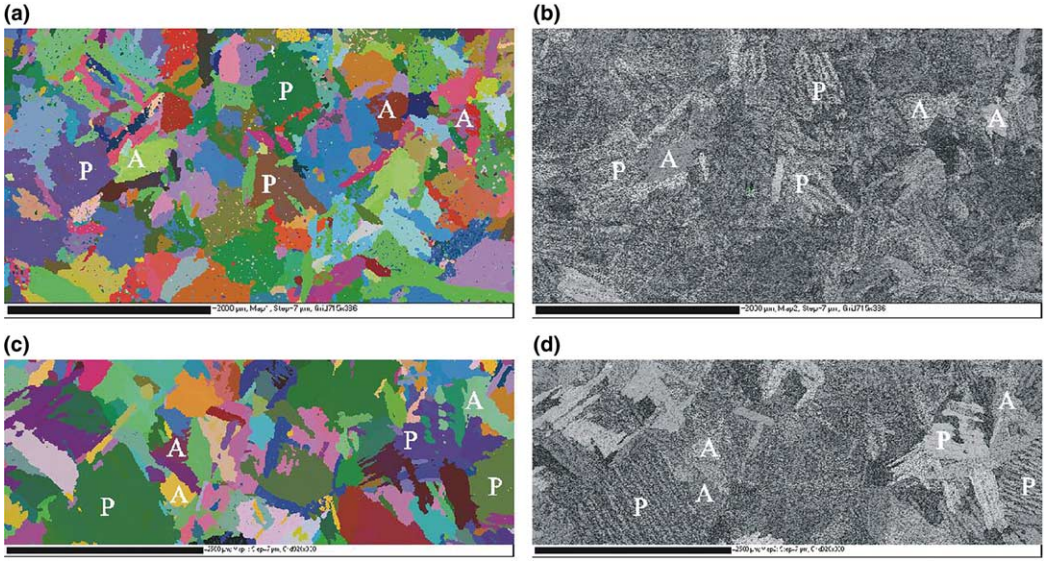

Fig. 12. EBSD map data from (a) and (b) surface and (c) and (d) internal section of ex situ transformed Ti slab material, with areas of plates (P) and allotriomorphs (A). (a) and (c) Colour coded crystallographic orientation data, highlighting the similarity in microstructure, with domains showing complicated grain boundary geometry and grain sizes frequently >1 mm diam. (b) and (d) Maps of variation in diffraction pattern quality. Grain boundaries or internally strained areas often show less intense diffraction and thus this parameter is used to highlight subtle substructure within domains, such as packets of plates with similar orientation (P).

phase grain-size can be inferred. The transient growth process observed in situ at the initial stage of the α–β transformation leaves no record in the α–β–α samples transformed ex situ, and thus the effect of the free surface on this phenomenon is difficult to assess. However, it can be deduced from Figs. 12(b) and (d) that α plates and allotriomorphs in these samples, nucleate not only at the free surface but also within the volume. In the in situ experiments it is possible that nucleation and growth occur at lower driving forces because the free surface assists these processes; however, the microstructural observations appear to be at least qualitatively similar at the surface and within the sample volume.

A comparison of the microtexture of the two microstructures in Fig. 12 is shown in the contoured pole figures of Fig. 13. Visual inspection of the pole figure indicates that the distribution of orientations in the two sections is very similar, indicating that there is not a significant effect from the free surface. A rigorous calculation of the β phase microtexture is not possible due to variant selection in the β–α transformation. However, assuming the Burgers OR is obeyed, it is possible to show that the dominant elements of the α texture are consistent with a combination of $(0\,0\,1)\langle 1\,0\,0\rangle$ and $(1\,1\,2)\langle 1\,1\,1\rangle$ texture components observed in this contribution and reported by others [9,10], these β phase orientations are superimposed on the α phase pole figure.

The unique advantage of the in situ approach is that it provides direct observation of the transient processes involved in the α–β transformation. Ultimately, these observations should improve our ability to predict, and

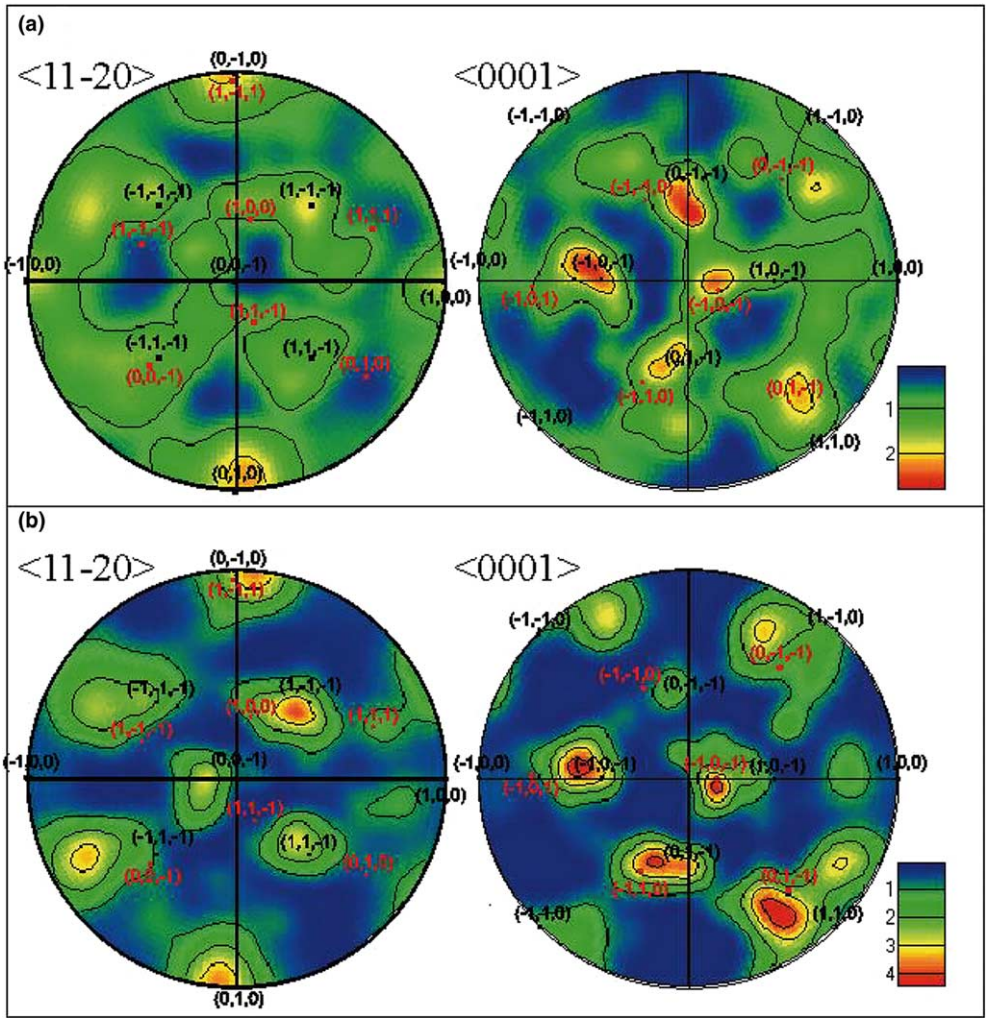

Fig. 13. Contoured pole figures showing the crystallographic texture of (a) surface and (b) internal section of ex situ transformed Ti slab material. Visual inspection of the distribution of orientations shows that a similar texture is developed at the surface and internally. Reconstruction of the β texture from the inherited α texture is problematic (due to variant selection in the β–α transformation); however, the overlay of β orientations indicates that the α textures are consistent (assuming Burgers OR) with the $(0\,0\,1)\langle 1\,0\,0\rangle$ and $(1\,1\,2)\langle 1\,1\,1\rangle$ components observed in the in situ experiments.

potentially control, microstructural development involving phase transformations.

5. Conclusions

In situ observations at temperatures above 900 °C of the α–β phase transformation in commercially pure titanium using SEM imaging concurrent with diffraction information via EBSD shows:

1. The β phase nucleates and grows at and along the α grain boundaries as allotriomorphs, and within the α grains as plates, with several variants usually occurring with one grain.
2. The intragranular plates have a Burgers OR with the parent α grain, are lenticular in shape and have a surface tent relief indicative of a military phase transformation mechanism. The intragranular plates have a habit plane in the vicinity of the specific {3 3 4} for a particular variant of the OR predicted by the PTMC for titanium.
3. The grain boundary allotriomorphs have a Burger OR with one of the α grains at the boundary, but do not possess a specific habit plane and do not have any apparent surface relief associated with them.
4. The phase transformation is completed via the consumption of the remaining α phase and all of the existing β plates by β allotriomorphs with more mobile boundaries, resulting in a large grained microstructure with a near-equilibrium triple junction arrangement. Grain growth in the β microstructure is at least an order of magnitude faster than in the α microstructure at similar temperatures.
5. The strong components in the β crystallographic texture determined at temperature can be correlated directly to the initial α texture via the Burger OR. However, a bias towards particular variant orientations shows that a variant selection process is occurring. Observation of multiple intragranular β plates within α parent grains suggests that the variant selection is not occurring in the early stages of transformation, but the recorded bias towards particular orientations is the result of preferred nucleation and/or growth of allotriomorphs.

Acknowledgements

We thank the Higher Education Funding Council for England (HEFCE) and the Natural Environment Research Council (NERC) for the provision of funds through the Joint Research Equipment Initiative (JREI) for the development of the CamScan 500X instrumentation. The author G.G.E.S. is grateful to The University of Liverpool and HEFCE for the student scholarship. S.C. and R.C.P. acknowledge the Engineering and Physical Sciences Research Council (EPSRC) for financial support.

References

[1] Humphreys FJ, Ferry M. Mater Sci Forum 1996;217–222:529.
[2] Springer F, Radomski M. Mater Sci Forum 1998;273–275:497.
[3] Seward GGE, Prior DJ, Wheeler J, et al. Scanning 2002;24:232.
[4] Elmer JW, Wong J, Ressler T. Metall Mater Trans A 1998;29:2761.
[5] Gey N, Humbert M, Philippe MJ, Combres Y. Mater Sci Eng A 1996;219:80.
[6] Wagner F, Bozzolo N, Van Landuyt O, Grosdidier T. Acta Mater 2002;50:1245.
[7] Furuhara T, Maki T. Mater Sci Eng A 2001;312:145.
[8] Burgers WG. Physica 1934;1:561.
[9] Zhu ZS, Gu JL, Liu RY, Chen NP, Yan MG. Mater Sci Eng A 2000;280:199.
[10] Gey N, Humbert M. Acta Mater 2002;50:277.
[11] Prior DJ, Trimby PW, Weber UD. Mineralog Mag 1996;60:859.
[12] Dingley DJ, Field DP. Mater Sci Technol 1997;13:69.
[13] Day AP, Quested TE. J Microsc 1999;195:186.
[14] Humphreys FJ, Hatherly M. Recrystallization and related annealing phenomena. Oxford: Pergamon Press; 1995.
[15] Hirth JP, Pond RC. Acta Metall Mater 1996;44:4749.
[16] Christian JW. The theory of transformations in metals and alloys. Oxford: Pergamon Press; 2002.
[17] Hirth JP, Spanos G, Hall MG, Aaronson HI. Acta Mater 1998;46:857.
[18] Bowles JS, Mackenzie JK. Acta Metall 1954;2:129.
[19] Wechsler MS, Lieberman DS, Read TA. Trans AIME 1953;197:1503.
[20] Wayman CM. Introduction to the crystallography of martensite transformations. New York: Macmillan; 1964.
[21] Mackenzie JK, Bowles JS. Acta Metall 1957;5:137.
[22] ASM Handbook. Ohio: America Society of Metals.
[23] Pond RC, Celotto S. Int Mater Rev 2003;48:225–45.
[24] Pond RC, Celotto S, Hirth JP. Acta Mater 2003;51:5385–98.